ISSN 1063-7826, Semiconductors, 2017, Vol. 51, No. 4, pp. 444–448. © Pleiades Publishing, Ltd., 2017.
Original Russian Text © M.I. Vexler, Yu.Yu. Illarionov, I.V. Grekhov, 2017, published in Fizika i Tekhnika Poluprovodnikov, 2017, Vol. 51, No. 4, pp. 467–471.

SEMICONDUCTOR STRUCTURES, LOW-DIMENSIONAL SYSTEMS, AND QUANTUM PHENOMENA

Quantum-Well Charge and Voltage Distribution in a Metal–Insulator–Semiconductor Structure upon Resonant Electron Tunneling

M. I. Vexler[a]*, Yu. Yu. Illarionov[a, b], and I. V. Grekhov[a]

[a] *Ioffe Physical–Technical Institute, Russian Academy of Sciences, St. Petersburg, 194021 Russia*
[b] *Technische Universität Wien, Institut für Mikroelektronik, Vienna, Gußhausstr. 29, A-1040 Austria*
**e-mail: vexler@mail.ioffe.ru*

Submitted November 1, 2016; accepted for publication November 10, 2016

Abstract—The prerequisites for electron storage in the quantum well of a metal–oxide–p^+-Si resonant-tunneling structure and the effect of the stored charge on the voltage distribution are theoretically investigated. Systems with SiO_2, HfO_2, and TiO_2 insulators are studied. It is demonstrated that the occurrence of a charge in the well in the case of resonant transport can be expected in structures on substrates with an acceptor concentration from (5–6) × 10^{18} to (2–3) × 10^{19} cm^{-3} in the range of oxide thicknesses dependent on this concentration. In particular, the oxide layer thickness in the structures with SiO_2/p^+-Si(10^{19} cm^{-3}) should exceed ~3 nm. The electron density in the well can reach ~10^{12} cm^{-2} and higher. However, the effect of this charge on the electrostatics of the structure becomes noticeable only at relatively high voltages far above the activation of resonant transport through the first subband.

DOI: 10.1134/S1063782617040224

1. INTRODUCTION

Resonant tunneling (RT) in metal–insulator–semiconductor (MIS) structures is a relatively new aspect in their physics. Electron transport of this type can be implemented when the bottom E_i of at least one subband of the near-surface quantum well (QW) is lower in energy than the edge $E_{v\infty}$ of the valence band (v band) of the bulk of a semiconductor (Fig. 1). At an acceptor concentration of N_A ~10^{19} cm^{-3} in Si and nanometer-range oxide thicknesses, silicon and oxide barriers are fairly transparent for the RT of electrons in the v-band–QW–metal path.

This phenomenon was studied by us in [1, 2]. In [2], we managed to demonstrate that under certain conditions, RT is accompanied by the occurrence of a mobile carrier charge in the QW. However, questions about the exact values of this charge and about the extent of its effect on the voltage distribution remain unanswered. In this study, we theoretically investigate the quantitative part of the effect of electron charge storage in different modes in metal–oxide–p^+-Si structures.

The investigated situation recalls the case of refilling the QW by means of interband tunneling at very large band bending in Si, which can take place independent of RT [3] and even in the case of not very heavy doping. This case is beyond our study; in our opinion, it is more interesting to analyze the case where the QW starts to be refilled already upon RT activation through the first subband, i.e., at $E_{c0} + E_1 \sim E_{v\infty}$ and at low biases.

2. FUNDAMENTALS OF THE MIS STRUCTURE MODEL UNDER RESONANT TUNNELING CONDITIONS

Since the tunnel MIS structure theory has been developed fairly well and published [4, 5], here we consider only the items important for RT.

The energy levels in the QW can be determined from the quasiclassical relation

$$\int \sqrt{E_c(z) - E_i}dz = \frac{\pi\hbar}{\sqrt{2m_{i,z}}}\left(n - \frac{1}{4}\right), \qquad (1)$$

where $E_c(z)$ is the conduction-band (c band) profile and the value 1/4 in parenthesis reflects the closeness of the QW shape to triangular [6]. The first level E_1 corresponds to “heavy” electrons ($E_{he,\,1}$, $n = 1$, and $m_i = m_{he}$) and the second level E_2 corresponds to the second “heavy” ($E_{he,\,2}$, $n = 2$, and $m_i = m_{he}$) or the first “light” ($E_{le,\,1}$, $n = 1$, and $m_i = m_{le}$) subbands [6] (Fig. 1).

The current filling the QW consists of the thermal generation current j_d and the band-to-band tunneling

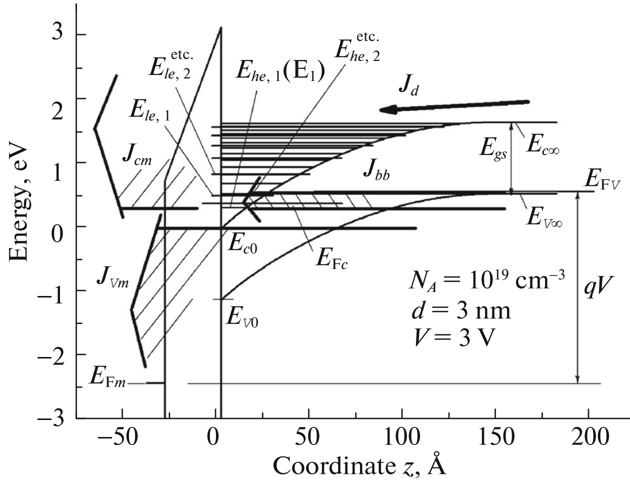

Fig. 1. Energy-band diagram of an Al/SiO_2/p^+-Si(100) MIS structure. The mode corresponds to the situation where level E_1 is involved in RT and levels E_{he2} and E_{le1} are at the edge of involvement. After taking into account charge storage in the QW by means of RT, the QW Fermi energy E_{Fc} is only slightly lower than E_{FV} (without storage, the difference $E_{FV} - E_{Fc}$ would be noticeably larger).

current j_{bb} (Fig. 1). The behavior of the current j_{bb} is determined by the subsequent involvement of levels E_i of the well in transport. In the stationary case, QW filling is balanced by electron leakage j_{cm} to the metal. The current j_d is small in itself (~10^{-10} A/cm^2) and as compared with the other components in the modes of our interest.

The electron densities N_i at the levels E_i of the QW are distributed in accordance with the Fermi function $f_c(E, E_{Fc})$. These densities and the Fermi energy E_{Fc} of the QW are determined from the conditions of the balance of the resulting electron appearance and escape currents

$$j_{cm} = \frac{q}{\pi\hbar^2}\sum_{E_i}\frac{\zeta_i m_{i\perp}}{\tau_{ar,i}}\int(f_c - f_m)T_{ox}dE$$
$$= \frac{q}{\pi\hbar^2}\sum_{E_i<q\varphi_s<E_{gs}}\frac{\zeta_i m_{i\perp}}{\tau_{ar,i}}\int(f_v - f_c)T_s dE + j_d \quad (2)$$
$$= j_{bb} + j_d,$$

$$N_i = \frac{\zeta_i m_{i\perp}k_B t}{\pi\hbar^2}\ln\left[1 + \exp\frac{E_{Fc} - E_i}{k_B t}\right]. \quad (3)$$

Here, $T_{ox|s} = T_{ox|s}(E, E_\perp)$ is the probability of the tunneling of an electron with the total energy E and the transverse energy $E_\perp = E - E_i$ through the oxide (ox) or Si (s) barriers; $f_{v|c|m}(E, E_{Fv|c|m})$ is the Fermi function in the bulk of p^+-Si (v), the QW (c), and the metal (m); $\tau_{ar,\ i}$ is the time of back and forth electron passage through the QW; m_i and ζ_i are the effective mass and degeneracy for the level E_i; t is the temperature (300 K); and $q\varphi_s$ is the Si band bending. The sum ΣN_i yields the total two-dimensional electron density N_s in the well.

In addition, the current j_{cm} is added to the current j_{vm} of nonresonant transport from the Si v band to the metal with energies below the QW (Fig. 1): $j = j_{cm} + j_{vm}$.

We use the following parameters of the tunnel barriers: pemittivities of $\varepsilon_s = 11.9$ (Si) and $\varepsilon_{ox} = 3.9$ (SiO_2), 25 (HfO_2), and 80 (TiO_2) and c-band offsets at the Si/oxide interface of $\chi_e = 3.15$ (SiO_2), 1.4 (HfO_2), and 1.2 eV (TiO_2) [7]. The effective electron masses in Si(100) and degeneracy were $m_{he,\ z} = 0.916m_0$, $m_{he\perp} = 0.19m_0$, $\zeta_{he} = 2$, and $m_{le,\ z} = 0.19m_0$, $m_{le\perp} = 0.417m_0$, $\zeta_{le} = 4$. The electron effective mass is $0.42m_0$ in SiO_2 [5], $0.15m_0$ in HfO_2, and $0.5m_0$ in TiO_2 [8–10]. The probabilities T_s and T_{ox} are determined by the Wentzel–Kramers–Brillouin method [5]; RT was correctly taken into account using formula (2).

3. OCCURRENCE OF CHARGE IN THE QUANTUM WELL UNDER RESONANT TUNNELING: OBSERVATION AND CONDITIONS

To warrant charge storage, the barrier ratio in the MIS system should be such that the input (semiconductor) barrier is more transparent than the output (oxide) barrier. Mathematically, it is expressed by the inequality $T_s > T_{ox}$; then, to equalize the input and output currents in the QW, it is necessary to raise the quasi-Fermi level E_{Fc} of the QW and shift it toward E_{Fv}. In the opposite case [1], the inequality $T_s < T_{ox}$ was valid and the level E_{Fc} was located much lower than E_{Fv}.

3.1. Experimental Facts

The occurrence of a charge in the QW can be experimentally observed by comparing the onward and return traces of the current–voltage I–V characteristic at the blocking polarity (+ at Al). The I–V characteristic should have steps at voltages V_1, V_2, ..., each corresponding to the involvement of the next subband with the bottom E_i in RT [1, 2]. The onward portion always looks like that (Fig. 2). However, at sufficiently fast recording (even at ~1 V/min), the I–V characteristics of the structures with relatively thick (~3 nm and more) SiO_2 with inclusion of the voltage range above the activation threshold V_1 of the level E_1, the return trace does not repeat the onward one (Fig. 2). At the same time, for samples with a thin oxide, the onward and return portions completely coincide. This can be attributed to the presence in the first case of an electron charge in the QW whose dissolution requires a finite time. The oxide layer in the investigated samples was formed by thermal oxidation

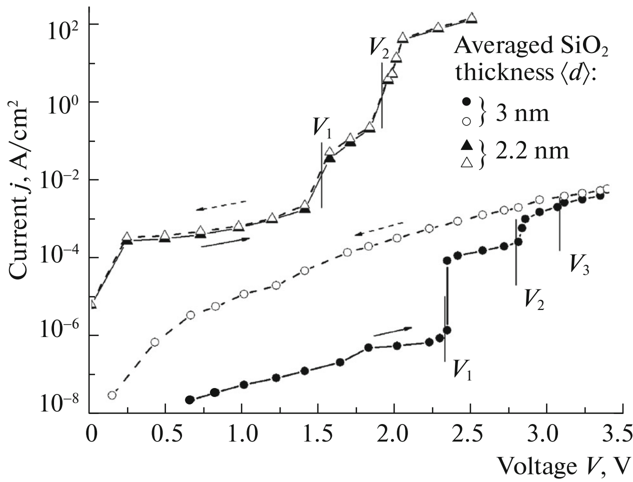

Fig. 2. Experimental I–V characteristics of the MIS structures $Al/SiO_2/p^+$-Si(100) with $N_A \sim 10^{19}$ cm^{-3} (blocking polarity). At a rather large insulator thickness, hysteresis caused by the occurrence of charge in the QW due to RT is observed.

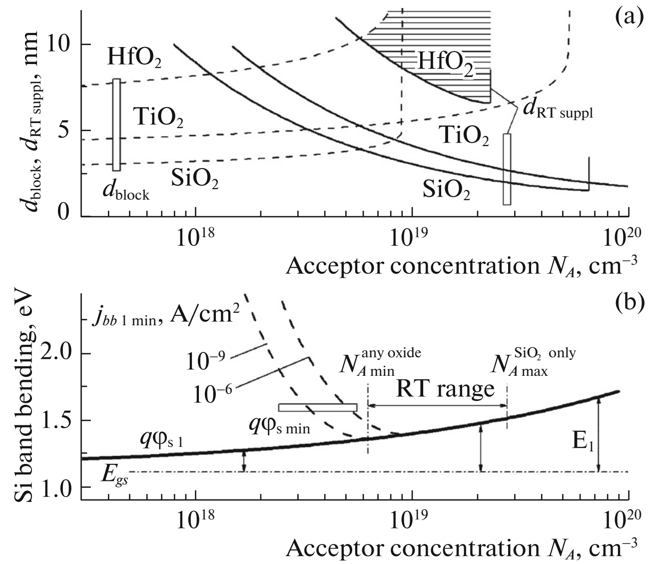

Fig. 3. (a) Calculated insulator layer thicknesses $d_{RT\,suppl}$ for the metal/oxide/Si(100) structures at which the oxide layer becomes less transparent for RT than the semiconductor layer, and the thicknesses d_{block} at which the thermal generation current exceeds possible leakage through the oxide. The region of variation in the parameters corresponding to RT with charge storage is shown (hatched) by the example of HfO_2. (b) Bending of bands $q\varphi_{s1}$ upon RT activation and its value $q\varphi_{s1\,min}$ necessary for the v-band–well current flow.

in dry oxygen. A similar I–V characteristic with hysteresis was obtained by us in [2] for samples with an electrochemical oxide.

It is no surprise that storage is typical of thick structures, since they are characterized by the relation $T_s \gg T_{ox}$ between the barrier tunnel transparencies. Certainly, such an experiment only allows us to claim the occurrence of charge in the QW without answering the question on the degree of its effect on the voltage distribution in the structure. This question needs to be theoretically analyzed.

3.2. Parameters of the Structures with Charge Storage

Figure 3 shows the calculated minimum oxide thicknesses $d_{RT\,suppl}$ at which the QW can be refilled by means of RT: under the RT activation conditions $V = V_1$ (or for band bending in silicon $\varphi_s = \varphi_{s1}$), the transparency relation will become $T_s(E_1, 0) > T_{ox}(E_1, 0)$. In the calculation, we used the depletion model acceptable in pre-activation modes. However, when the thickness d exceeds some value d_{block}, this model is not quite valid, since the storage of electrons in the MIS structure can be caused by a thermal current j_d without RT. The $d_{block}(N_A)$ dependences (at the criterion that under the condition $\varphi_s = \varphi_{s1}$ without RT at $d = d_{block}$ the QW charge amounts to 1% of the total charge in Si) are also presented in Fig. 3.

As a result, the occurrence of a charge in the QW by means of RT should be expected in the region $d_{RT\,suppl} < d < d_{block}$. The break of the $d_{RT\,suppl}(N_A)$ curves for SiO_2 and HfO_2 on the side of high N_A values suggests that, upon excessive doping, the probability T_{ox}, which depends, in this case, only on the field in the oxide, will exceed T_s at any d and a break in the $d_{block}(N_A)$ curves indicates that the thermal current will not lead to storage at any d.

For the structure to be interesting in studying charge in the QW under RT, in addition to the validity of the condition $T_s > T_{ox}$, the current j_{bb1} between the v band and subband *1* should be noticeable, i.e., not lower than 10^{-9}–10^{-6} A/cm^2. Figure 3b shows the band bendings $q\varphi_{s\,1}$ in Si that correspond to RT activation and the bending $q\varphi_{s\,min}$ in the depletion model at the current $j_{bb1} = j_{bb1\,min}$ to subband *1*. The obvious excess of $q\varphi_{s\,min}$ over $q\varphi_{s\,1}$ is indicative of the weakness of RT in a system; this excess occurs at the insufficient acceptor concentration N_A. However, as we see, this limitation does not introduce any drastic changes: the boundary $N_{A\,min}$ is close to the abscissas of the points of intersection of the $d_{RT\,suppl}$ and d_{block} curves in Fig. 3a. On the other hand, when the concentration N_A is too high, the field in the oxide will exceed the breakdown field; this determines the right-hand boundary of the range $N_{A\,min}...N_{A\,max}$. The limitation via $N_{A\,max}$ is important for SiO_2 (indicated as the RT range) and is apparently less important for HfO_2 or TiO_2: the breakdown field F_{br} of high-k materials is lower than in SiO_2 ($F_{br} \sim 10^7$ for SiO_2, $\sim 5 \times 10^6$ for

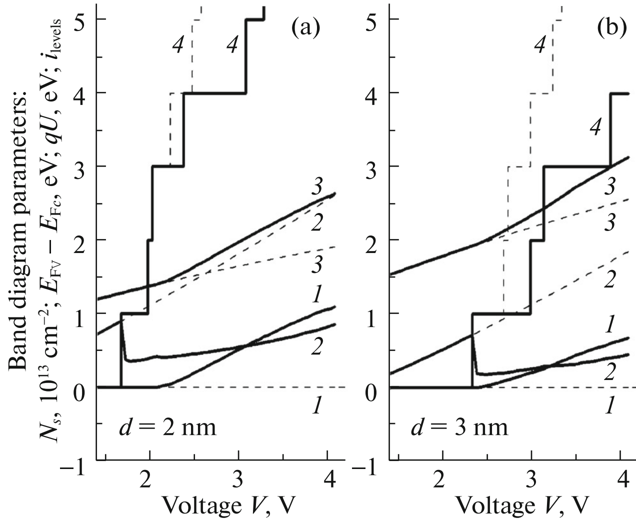

Fig. 4. Calculated details of the energy band diagram of the $Al/SiO_2/p^+$-Si(100) MIS structure with $N_A \sim 10^{19}$ cm^{-3} at oxide thicknesses of (a) d = 2 and (b) 3 nm, against the voltage. Solid lines are plotted taking into account the effect of RT on the electron charge in the QW and dashed lines are plotted under the assumption that the well is refilled only by means of thermal generation in the bulk of Si. (*1*) N_s, (*2*) $E_{Fv} - E_{Fc}$, (*3*) qU, and (*4*) i_{levels}.

HfO_2 [11], and $\sim 10^6$ V/cm for TiO_2 [12]), but by a factor smaller than the permittivity ratio.

In the analysis, we use φ_{s1} instead of V_1 because this quantity (or the related depletion region width w_1) is more universal as long as the QW of the MIS structure contains a small number of carriers. The voltage V_1, in turn, is mediated by the work function of the metal, as well as by insulator thickness and permittivity. Recalculation is simple, taking into account the equality $V_1 = V_{FB} + U_1 + \varphi_{s1}$, where $U_1 = qN_Aw_1d/\varepsilon_0\varepsilon_{ox}$, $\varphi_{s1} = qN_Aw_1^2/2\varepsilon_0\varepsilon_s$, and V_{FB} is the voltage corresponding to flat bands.

4. EFFECT OF CHARGE ON DETAILS OF THE ENERGY BAND DIAGRAM

4.1. The Effect in a Wide Voltage Range

The appearance of electrons in the QW can change many parameters as compared with the results obtained using the depletion model, employed by us previously [1] for a thin oxide barrier. These parameters are the charge concentration N_s (cm^{-2}), quasi-Fermi-level position in the well (E_{Fc}) with respect to the Fermi levels in the bulk of Si and metal (E_{Fv} and E_{Fm}), and details of the energy-band diagram, including the distribution of the applied voltage $V = q^{-1}(E_{Fv} - E_{Fm})$ between the oxide, U, and the substrate, φ_s. These changes shift the activation voltages V_i of levels E_i, starting with the second one.

Figure 4 shows the calculated dependences of N_s, U, and $E_{Fv} - E_{Fc}$ and the number of levels i_{levels} involved in RT on the bias V for two silicon dioxide thicknesses. The presented curves are obtained with regard to QW refilling by means of RT and without it taken into account. Disregarding storage means that only a small number of carriers drifting over the Si c band enters the QW; i.e., this process does not provide a noticeable electron density at the chosen d values, yet somewhat enhances E_{Fc}.

We can see that the QW charge can attain quite noticeable values ($>10^{12}$ cm^{-2}) and significantly affect many components of the energy band diagram. The relative effect of this charge increases with the voltage V applied to the structure. The sharp approach of E_{Fc} to E_{Fv}, which is reflected in an abrupt drop in the difference $E_{Fv} - E_{Fc}$, occurs directly during activation.

4.2. Effect in the Modes Close to RT Activation

The modes close to $V = V_1$ are of special interest, since, in this case, the RT phenomena should manifest themselves to the highest extent. To estimate the scale of the QW charge effect in these modes, we should take into account that the highest concentration N_s of the charge supported by RT from the v band at the specified voltage V can be attained at $E_{Fc} \rightarrow E_{Fv}$, i.e., in the limit of quasi-equilibrium in the substrate. If we determine the electric field F_{equil} in the oxide at $V = V_1$ in the equilibrium MIS structure and field F_{depl} at the same voltage in the depletion model, then the ratio $(F_{equil} - F_{depl})/F_{depl}$ will yield the upper estimate of the QW charge effect in the structure with this insulator material of specified thickness d. This ratio will be the largest at the highest ε_{ox} values.

We can conclude from the data illustrated in Fig. 5 that, in the investigated voltage range, the effect of charge storage in the QW on the energy band diagram is insignificant. The role of storage increases with a decrease in the dopant concentration N_A, but the RT process is then very weak. In real doping situations ($N_A \sim 10^{19}$ cm^{-3}), the relative contribution of the QW charge is not larger than 10% or even units of percent. Thus, the only noticeable consequence of the charge qN_A is sharp growth of the quasi-Fermi level E_{Fc} in the QW (and, correspondingly, a drop in $E_{Fv} - E_{Fc}$, see Fig. 4). Therefore, if in some problem only the range near the activation moment V_1 is important, then the depletion model can be used to calculate the band profile and the well charge qN_s and E_{Fc} can be found for the available band diagram. This simplifies the calculations, since makes it possible to avoid additional iterations.

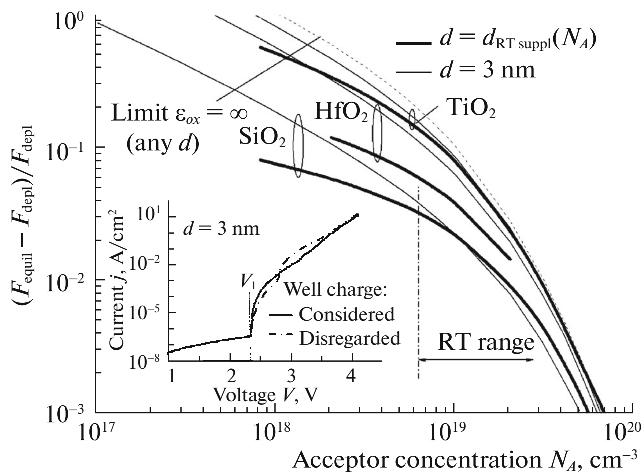

Fig. 5. Estimation of the maximum possible effect of QW charge on the voltage distribution in the metal/oxide/Si(100) structure with $N_A \sim 10^{19}$ cm^{-3}: comparison of electric fields in the oxide at the transition from depletion to equilibrium in the MIS structure at $V = V_1$. The right-hand side of the real RT range is determined by the insulator material. The inset: I–V characteristics calculated with regard to the well charge and without it taken into account.

The inset in Fig. 5 shows the currents calculated for the MIS structure with regard to QW charge appearance under RT and without it taken into account. As for the electric field, we can state that near $V = V_1$ taking the QW charge into account is not fundamentally important, since its role becomes more noticeable at $V \sim 3$ V, i.e., already in the region far from that corresponding to the instant of activation of the first subband.

5. CONCLUSIONS

This study showed that resonant electron tunneling in MIS structures can lead to the occurrence of a noticeable ($\sim q \times 10^{12}$ cm^{-2} and larger) charge in the surface quantum well. The conditions for the occurrence of this charge are (i) exceeding the tunnel transparency of the oxide barrier by that of the semiconductor barrier, (ii) the weak thermal generation of electrons, (iii) sufficient (in terms of absolute value) current from the valence band to the well, and (iv) field values below breakdown in the insulator. We presented the specific limits of doping and insulator film (SiO_2, HfO_2, and TiO_2) thickness ranges where we should expect charge storage. The available experimental data confirm that the charge phenomena are typical of structures with relatively thick oxide films. The stored charge can affect the energy-band diagram of the MIS structure. However, the distortions introduced by this charge manifest themselves in modes far from the voltage V_1 of activation of the first resonance level. At bias voltages somewhat higher than V_1 (this is the most interesting region), the voltage distribution can be calculated using the depletion model; after that, the charge of the well and position of its quasi-Fermi level are determined.

REFERENCES

1. G. G. Kareva and M. I. Vexler, Semiconductors **47**, 1084 (2013).
2. M. I. Vexler, G. G. Kareva, Yu. Yu. Illarionov, and I. V. Grekhov, Tech. Phys. Lett. **42**, 1090 (2016).
3. B. Eitan, P. Pavan, I. Bloom, A. Efraim, A. Frommer, and D. Finzi, IEEE Electron Dev. Lett. **22**, 543 (2000).
4. A. Schenk, *Advanced Physical Models for Silicon Device Simulations* (Springer, Wien, New York, 1998), Chap. 5.
5. M. I. Vexler, S. E. Tyaginov, Yu. Yu. Illarionov, Yew Kwang Sing, Ang Diing Shenp, V. V. Fedorov, and D. V. Isakov, Semiconductors **47**, 686 (2013).
6. T. Ando, A. Fowler, and F. Stern, *Electronic Properties of Two-Dimensional Systems* (Mir, Moscow, 1985); Rev. Mod. Phys. **54**, 437 (1982), Chap. 3.
7. J. Robertson and R. W. Wallace, Mater. Sci. Eng. Res. **88**, 1 (2015).
8. S. Monaghan, P. K. Hurley, K. Cherkaoui, M. A. Negara, and A. Schenk, Solid State Electron. **53**, 438 (2009).
9. B. Govoreanu, P. Blomme, K. Henson, J. van Houdt, and K. de Meyer, in *Proceedings of the Conference on Simulation of Semiconductor Processes and Devices SISPAD, Boston, USA, Sept. 3–5, 2003,* p. 287.
10. Y. Rawal, S. Ganguly, and M. S. Baghini, Active Passive Electron. Compon. **2012**, 694105 (2012).
11. L. Kang, B. H. Lee, W.-J. Qi, Y. Jeon, R. Nieh, S. Gopalan, K. Onishi, and J. C. Lee, IEEE Electron Dev. Lett. **21**, 181 (2000).
12. L. Zhou, R. C. Hoffmann, Z. Zhao, J. Bill, and F. Aldinger, Thin Solid Films **516**, 7661 (2008).

Translated by E. Bondareva